*energies*

MDPI

*Review*

# Silicon–Germanium: The Legacy Lives On

**Bruce Cook**

Material Dynamics & Devices, Inc., Raleigh, NC 27603, USA; bruce@matdd.com

**Abstract:** Alloy systems comprised of silicon with germanium, lead with tellurium, and bismuth with antimony have constituted a majority of thermoelectric applications during the last half-century. These legacy materials are primarily covalently bonded with a maximum *ZT* near one. Silicon–germanium alloys have provided the thermal to electrical conversion for many of NASA's radioisotope thermoelectric generator (RTG) configurations and for nearly all of its deep space and outer planetary flights, such as Pioneer I and II, Voyager I and 11, Ulysses, Galileo, and Cassini. The remarkable success of these materials and their respective devices is evidenced by the fact that there has never been a failure of the RTG systems even after over 1 billion cumulative mission-hours. The history of this alloy system as a thermoelectric conversion material spans over six decades and research to further improve its performance continues to this day. Si-Ge alloys have long been a mainstay of thermoelectric research because of a fortuitous combination of a sufficiently high melting temperature, reasonable energy band gap, high solubility for both n- and p-type dopants, and the fact that this alloy system exhibits complete miscibility in the solid state, which enable tuning of both electrical and thermal properties. This article reviews the history of silicon–germanium as a thermoelectric material and its use in NASA's RTG programs. Since the device technology is also a critical operational consideration, a brief review of some of the unique challenges imposed by the use in an RTG is also discussed.

**Keywords:** silicon–germanium; RTG; thermoelectric material processing



**Citation:** Cook, B. Silicon–Germanium: The Legacy Lives On. *Energies* **2022**, *15*, 2957. https://doi.org/10.3390/en15082957

Academic Editors: Bertrand Lenoir, Terry J. Hendricks, Thierry Caillat and Takao Mori

Received: 2 March 2022
Accepted: 14 April 2022
Published: 18 April 2022



## 1. Introduction

To say that silicon–germanium has proven itself as one of the most reliable high-temperature thermoelectric materials is an understatement. The history of this alloy system as a thermal-to-electrical conversion material spans over six decades and research to further improve its performance continues to this day. Beginning with LES-8 and LES-9 satellites launched back in the mid-1970s, Si-Ge has been the workhorse for radioisotope power. While the Voyager 1 and 2 probes have received notoriety for their robust longevity, it is worth noting that LES-9 was the longest continuously operating communications satellite in U.S. history, operating from its launch in 1976 until it was decommissioned by MIT Lincoln Laboratory on 20 May 2020. The two Voyager spacecraft, both launched in 1977, have accumulated nearly 1 billion device-hours during their 44+ year journey, and as of early 2022 still continue transmitting data, albeit at a reduced power level from the natural decay of their radioisotope heat sources [1]. It is likely that sometime in the 2024–2025 time frame there will be insufficient power to maintain antenna alignment with earth, at which point communication with the spacecraft will be lost. Since the launch of the LES satellites and the Voyagers, based on the multi-hundred watt RTG design [2], several other historic planetary missions have successfully completed their objectives thanks to the reliability of Si-Ge thermoelectric materials in the larger GPHS-RTG, including Galileo, Ulysses, Cassini, and New Horizons.

## 2. The Thermoelectric Process

This section begins with a brief overview of the thermoelectric process in general and a background on silicon–germanium alloys in particular, followed by a review of

the components that make up the Si-Ge unicouples employed in the RTG missions. The thermoelectric effect is recognized as a fundamental electro-thermal property of matter, which is described by the dimensionless figure of merit, $ZT$;

$$ZT = \frac{S^2 \sigma T}{\lambda} \tag{1}$$

where $S$ is the Seebeck coefficient (sometimes referred to as thermopower [3]), $\sigma$ is the electrical conductivity, $\lambda$ is the total thermal conductivity, and T is the absolute temperature. This expression is derived from a thermodynamic analysis of energy conservation in a thermoelectric heat engine operating between $T_h$ and $T_c$. It represents the irreversible heat losses, which reduce the efficiency of such a thermoelectric material from the ideal Carnot value of $(T_h - T_c)/T_h = 1 - T_c/T_h$, in which the Carnot efficiency is maximized for the largest possible temperature difference. The relationship between the input heat to electrical conversion efficiency, $\eta$, and the quantity $ZT$ is given in Equation (2).

$$\eta = \frac{T_h - T_c}{T_h} \frac{\sqrt{1 + (ZT)_{ave}} - 1}{\sqrt{1 + (ZT)_{ave}} + \frac{T_c}{T_h}} \tag{2}$$

in which the subscript "*ave*" refers to the integrated average ($ZT$) over the specific temperature range of interest. This method of calculating efficiency is more realistic then the common approach of calculating efficiency only under condition of optimal resistive loading, e.g., at the point of maximum efficiency. Equation (2) shows that the efficiency increases as the quantity $(1 + ZT)^{\frac{1}{2}}$ is increased. As the quantity $ZT$ increases, the efficiency of the conversion process approaches the Carnot limit corresponding to the respective hot and cold junction temperatures. Optimization of the energy conversion process in a thermoelectric couple requires achieving a large Seebeck coefficient along with a low electrical resistivity and a low thermal conductivity.

There is no thermodynamic limit to $ZT$; theoretically, a material could exhibit an arbitrarily large $ZT$, which would simply mean its thermoelectric conversion efficiency would approach the Carnot value for a given temperature difference. The conventional semiconductor theory extends the analysis to fundamental materials properties, e.g., the best thermoelectric materials are those possessing high carrier mobility, low lattice thermal conductivity, and large effective mass. In order to prevent intrinsic conduction, which leads to a reduced thermopower and degradation of the thermoelectric properties, it is desirable that the intrinsic band gap of the material, $E_g$, be at least 4 to 5 kT, where T is the maximum expected operating temperature. For power generation devices operating in the 873 to 1273 K range, the band gap should be at least 0.7 eV. Along with solid solutions of Si and Ge, solutions of lead and tellurium comprise the best known and most widely-used bulk materials for RTG applications. The maximum $ZT$ in these legacy materials is near one and the chemical bonding in these alloys is primarily covalent. Considerable effort during the last two decades has gone into reducing thermal conductivity by various approaches. "Intrinsic" factors such as phonon–phonon and electron–phonon scattering are often augmented by "engineered" or "extrinsic" effects, such as mass and strain fluctuation, void fillers (rattlers), charge carriers from dopants, mixed-valence cations, grain boundaries, and precipitates. Phonon–phonon scattering gives rise to the familiar $T^{-1}$ dependence of thermal conductivity above the Debye temperature [4]. Phonon–electron scattering primarily affects the long wavelength, lower energy phonons, which have wavenumbers closest to that of the electrons. Point defect scattering, sometimes referred to as "mass fluctuation" scattering, refers to the scattering that occurs when a displacement wave encounters a zero dimensional (i.e., point) disruption in the periodicity of the lattice. For example, silicon and germanium exhibit complete miscibility and both have a chemical valency of four. However, their atomic masses are different, which leads to considerable mass fluctuation scattering of phonons. When one is substituted for another in a host

lattice, the electron scattering is minimal, while the difference in mass strongly scatters short wavelength phonons.

## 3. Si-Ge Alloys for RTG Applications

During the half-century in which Si-Ge has been employed in isotope power generation systems, the production of Si-Ge unicouples has undergone a number of stop and re-start cycles. Following completion of the MHW Si-Ge RTGs for the Voyager program, the Si-Ge thermoelectric production line at RCA was shut down as interest shifted to a new, higher efficiency generator design for the Galileo mission at 3 M based on an emerging class of copper-silver selenide and gadolinium selenide thermoelectric materials. Subsequent failure of the 3 M ground demonstration unit and disclosure of a deleterious phase transformation in the GdSe n-leg and excessive sublimation of the Cu-Ag-Se p-leg (driven by ionic conduction of the Cu atoms away from the hot junction), led to a Stop Work Order issued by DOE in January 1979 [5]. This left the Galileo program without a viable power source, which led to a restart of the Si-Ge program at GE-Valley Forge in 1979 and development of the higher-power GPHS-RTG for both Galileo and Ulysses. Following completion of Si-Ge unicouples for these missions, the production line was again shut down in 1984, only to be restarted in the late 1980s for Cassini. After production of unicouples for Cassini was completed in 1996 (and also spare unicouples that were eventually incorporated in the New Horizon mission), the Si-Ge production line at Valley-Forge, PA (USA) (then Lockheed Martin) was terminated.

### *Si-Ge Alloy Preparation and Device Architectures*

The basic science and feasibility studies on Si-Ge alloys were initially conducted at RCA's R&D Laboratory in Princeton, NJ, in ca. 1957. Within about 4 years from the decision to focus research on Si-Ge, the technology was transferred to an RCA operating division (Harrison, NJ, USA) where rudimentary, first-generation modules were fabricated and tested. In 1960, there were no TE materials that could operate above 773–873 K; however, by 1962 RCA had measured and published 7.3% efficiency in Si-Ge couples operating between 298–1140 K. It is interesting to note that the SNAP-10A satellite, launched in 1965, was the first mission to incorporate Si-Ge TE modules in its power system. A total of 100 modules were fabricated from zone leveled Si-Ge and the resulting device produced ~500 W of power at 30 V with the couples operating between 600 and 756 K (Figure 1) [6].

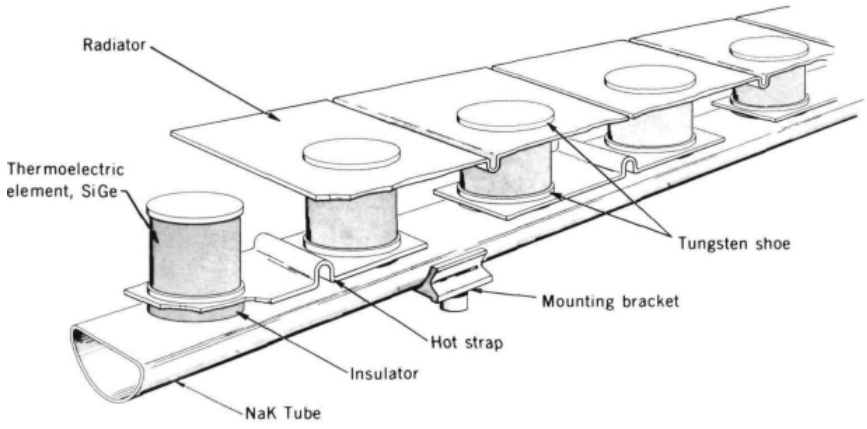


**Figure 1.** Schematic of first-generation Si-Ge couples used in the 1965 SNAP-10A mission.

The MHW and GPHS TE legs were comprised of 78 atomic percent silicon with a short 63.5 atomic percent section diffusion bonded at the cold end. The lower silicon content segment was used to improve matching for thermal expansion of the bonded parts. The n leg was doped with phosphorus and the p leg with boron. These materials were prepared by melting of the constituents followed by solidification in water-chilled copper finger

molds [7]. The 78 at. % Si composition was not arbitrarily chosen. It was known since the 1950s that silicon and germanium could both be chemically doped to increase electrical conductivity. However, the thermal conductivity of either element alone is far too high to be of use in thermoelectric applications. It was the insight of Abeles, Beers, Cody, and Dismukes at RCA Laboratories in the early 1960s during their study of point defects in semiconductors that led to the discovery of lattice thermal conductivity reduction by alloy scattering in the Si-Ge system [8,9]. Their work revealed a broad minimum in the thermal conductivity of the binary system between 20 and 90 at. % Si. The addition of dopants further reduces thermal conductivity through carrier–phonon scattering.

The development of silicon–germanium (Si-Ge) semiconductor alloys at RCA represented a major development in thermoelectric technology. Si-Ge enabled hot junction temperatures far exceeding the maximum temperature of other materials such as PbTe and TAGS. Si-Ge-based unicouple devices are mechanically robust and are unmatched by any other competitive thermoelectric material, even 50 years after the initial work on this alloy system. The remarkable performance characteristics of Si-Ge devices result from a combination of favorable physical properties, such as a high melting point (liquidus temperature in excess of 1573 K for the 78:22 composition [10]), ability to chemically dope at the levels necessary to achieve good TE figures-of-merit (~$10^{20}$ $cm^{-3}$ for both n- and p-type dopants), excellent strength properties with tensile strength values in excess of 7000 psi., exceptional shock-and-vibration resistance, lower weight than PbTe alloys (density = 3 $g/cm^3$), reasonable CTE, good bonding characteristics, and $ZT$ values approaching unity in the n-type composition.

Sublimation characteristics of the materials are well-understood and can be mitigated by a thin (1 micron) coating of $Si_3N_4$. Moreover, the degradation characteristics of doped Si-Ge follow well-behaved (i.e., predictable) metrics, enabling precise planning for long-term mission performance. While the Si-Ge alloy system exhibits complete miscibility, compositions within the range of 60–85 at. % silicon are preferred for TE applications because of the lower thermal conductivity resulting from a maximum in alloy scattering within this composition range and a sufficiently large band gap to minimize the onset of intrinsic conductivity. Moreover, the solid solubility of phosphorus (the n-type dopant) increases with increasing silicon content [11]. The net optimum composition falls in a range between 78 and 85 at. % Si. It was found by RCA that the addition of a short (3.18 mm) segment of lower Si content at the cold end provided for improved CTE matching with the W cold shoes.

The retrograde nature of the phosphorus solidus curve in Si-Ge creates some unique consequences. For example, an n-type alloy doped to saturation during melting, supersaturates at any lower temperature, and excess phosphorus precipitates out of solution with time. Because the number of charge carriers are in nearly a one-to-one correspondence with the phosphorus atoms in solid solution, both the Seebeck coefficient and the electrical resistivity are strongly affected by the precipitation of phosphorus. As a result, the transport properties of a cast, ground, and hot pressed n-type Si-Ge sample are not the equilibrium values; the values represent a dynamic transition between the supersaturated state and the equilibrium state. Equilibrium property values for heavily doped n-type materials also do not represent a constant doping level; the values reflect the change of equilibrium solid solubility with temperature. The net effect of dopant precipitation is an increase in both the Seebeck coefficient and the electrical resistivity. The degree of supersaturation and temperature both determine the rate and amount of precipitation. The initial rate is fairly rapid, but several thousand hours of aging result in the material approaching equilibrium. It should be mentioned that dopant precipitation also occurs in the boron-doped p-type Si-Ge alloys, only at higher temperatures. These effects are well-understood and documented [12–14].

Silicon and germanium are completely miscible in the solid-state, and since the two elements possess different melting temperatures, the Si-Ge binary phase diagram exhibits a miscibility gap that results in inhomogeneous solidification. Because of the wide separation between solidus and liquidus, most silicon–germanium compositions freeze out

with a cored microstructure (i.e., inhomogeneous). This can be thought of as silicon-rich cores surrounded by volumes of progressively higher germanium content. Equilibrium microstructures can only be achieved via extremely slow cooling rates.

In materials such as Si-Ge, the composition of the material that solidifies changes as the temperature is lowered. This produces a cored microstructure with inferior properties. Consequently, as-cast Si-Ge billets contain dendrites, or silicon-rich regions that are first to solidify when the melt composition passes through the liquidus. In other words, if one were to simply melt a mixture of Si and Ge and then cool down to room temperature, the result would be grains with a wide range of compositions, as illustrated in Figure 2.

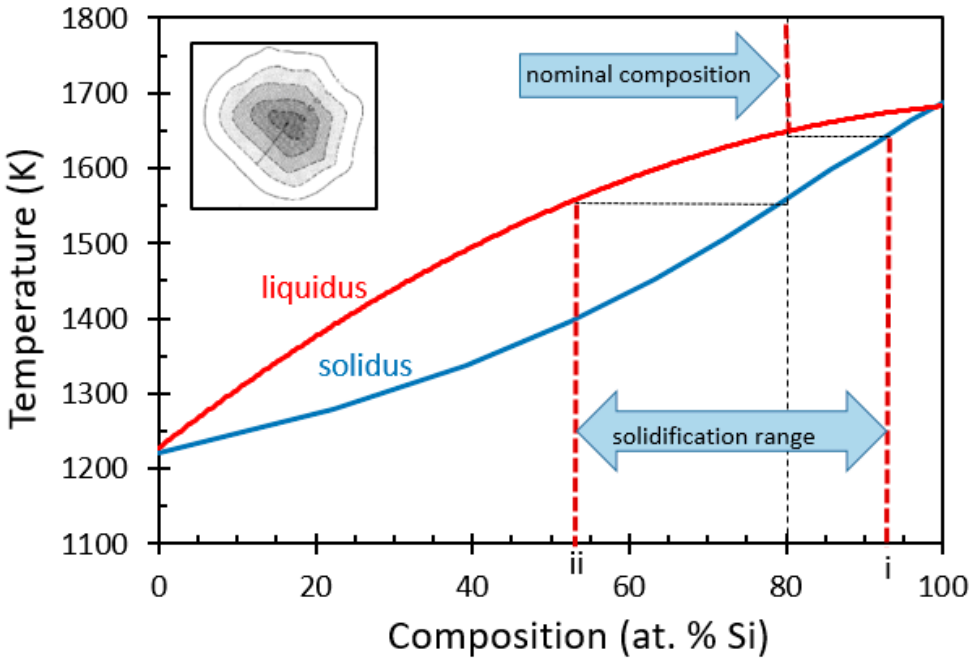


**Figure 2.** Binary equilibrium Si-Ge phase diagram showing solidification range for a nominal liquidus composition of Si-80% Ge-20% (atomic) [15]. (Typical cored microstructure is diagrammed in the insert). Composition "i" is the first solid to freeze-out; composition "ii" is the last solid to freeze-out.

With a nominal composition of 80 at. % Si, the first composition to freeze out during solidification is silicon-rich, with a composition of ~$Si_{90}Ge_{10}$. As the solidification progresses during cooling, these cored nuclei are surrounded by progressively higher germanium content volumes until the last solid phase freezes out with the nominal composition of 50 at. % Si. Such a cored microstructure would confer low mechanical strength and legs obtained from the casting would exhibit a range of transport properties and, thus, a range of *ZT* values. One solution is to maintain a fixed composition of the melt (i.e., zone leveling). This was used only once for the SNAP-10A generator in 1965. The resulting material is reasonably homogeneous but the process is slow and expensive; not amenable to large-scale production.

Vacuum melting combined with hot pressing provided an alternate solution. This process was employed for all Si-Ge production since the Voyager era. Hot pressing is simpler, faster, and less expensive than zone leveling. The process starts with alloy formation via melting in a fused silica crucible, followed by casting into water-cooled copper finger molds, grinding the casting into powder, and finally hot pressing the ground powder into dense compacts. Grinding reduces the diffusion distance for thermally-induced homogenization during hot pressing. The Cassini process included a second grinding and hot pressing sequence to improve the level of homogeneity. While hot pressing is considered the standard approach to powder consolidation, it also is fraught with potential pitfalls and nuances that can lead to unacceptable results, leading to low yields. For example,

the non-uniform distribution of densification within a hot pressed compact can produce distortion and crack formation during the compaction and ejection steps. The non-uniform density distribution is mainly due to the friction along the die wall. The presence of friction prevents the movement of powders downwards during the movement of upper punch. Consequently, powder near the bottom corners undergoes less compression while the powder near the top corners can reach nearly full theoretical density. The resulting pressure stress distribution within the compact results in non-uniform density. Die filling and cold pressing determine the uniformity of the green density in the powder compact, which is a critical process parameter. Green density gradients must be minimized in order to reduce differential shrinkage during sintering and shape distortion, as well as to avoid induced defects that limit the quality of the compact. The deleterious effects of differential springback [16] (which can lead to significant fracture and cracking in brittle materials such as Si-Ge) can be reduced by maintaining a small axial pressure on the compact during ejection (punch hold-down ejection or withdrawal of the die). A single-action hot press consists of one moving punch. While this can introduce high density gradients in the axial directions, compacts with a sufficiently low thickness to the diameter aspect ratio can be consolidated to 99% of theoretical density with negligible gradients if a suitable die-wall lubricant is employed. A double action press, as employed at Valley Forge during the Cassini program, has two independently moving punches that create a more uniform compaction especially for thicker compacts.

Beyond the issues associated with cored microstructures, there were other issues early on associated with chill casting of Si-Ge. One in particular involved the addition of the phosphorus dopant needed for the n-legs. Phosphorus has a high vapor pressure that causes loss of this constituent as the mixture of materials is initially heated. An acceptable workaround was to add phosphorus immediately before freezing the molten alloy, but that also resulted in significant loss as the phosphorus encountered the molten bath. The only solution was to add excess phosphorus so that a sufficient amount of the dopant remained when the casting was solidified. A process was eventually developed that could produce castings with a reproducible amount of dopant.

A third approach, developed for heavily-doped thermoelectric materials during the 1990s and subsequently adopted by numerous laboratories worldwide, involves forming the Si-Ge alloys by solid-state reaction near room temperature. This mechanochemical synthesis route avoids the dendritic segregation that is inherent in solidification synthesis and has the added benefit of eliminating the issue of loss of volatile dopants such as phosphorus. Mechanical alloying (MA) involves repeated welding, fracturing, and re-welding of powder particles in a high-energy reaction vessel. Originally developed to produce oxide-dispersion strengthened (ODS) nickel- and iron-based superalloys for applications in the aerospace industry, MA has been shown to be capable of synthesizing a variety of equilibrium alloy phases, starting from blended elemental constituents [17–21].

The results have been shown to be nearly identical with that of vacuum cast and hot pressed alloys [22,23]. Process variable affecting the final product include the effect of oxygen on $ZT$, control of contamination from milling media, constituent material form (powders vs. chunk), process atmosphere (vacuum vs inert), milling parameters (mass–charge ratio, input energy, duration), hot pressing parameters, and compact aspect ratio. Scaling up this technology to the kilogram quantities required for RTG applications has proven to be challenging since precise reproducibility in composition and microstructure is essential.

Synthesis of heavily-doped Si-Ge alloys as used in the legacy RTG unicouples becomes a “Goldilocks” problem: If the material is inhomogeneous, the material may not sinter uniformly and is likely to exhibit incipient melting, it will be mechanically weak, and the transport properties will not be predictable. Since charge carrier solubility and mobility are influenced by the Si:Ge ratio, distributions out of line with the “norm” can lead to “overdoping” or “underdoping” results. Out of “norm” distribution of grains in the compacts can influence the machining, cleaning and application of the $Si_3N_4$ coating.

Moreover, silicon-rich grains are more resistant to grinding and shatterboxing and, hence, can influence the particle size distribution in the hot pressed compacts. On the other hand if the material is highly homogeneous, the diffusion bonding process developed for the legacy materials (e.g., Cassini) would require modification since "standard" Si-Ge contained a small amount of Ge-rich material, which facilitated diffusion bonding to the SiMo hot shoes. Consequently, there exists a narrow window within which the compositional uniformity is just right; e.g., reasonably uniform but with a small amount of Ge-rich volumes.

Following the MHW and GPHS program eras, numerous groups around the world have studied modifications to silicon–germanium along with various processing routes to improve *ZT*. The study of grain-boundary scattering and the use of fine-grained alloys led to extensive use of hot pressing and spark plasma sintering to lower the lattice thermal conductivity. High-temperature heat treatments have been examined in order to alter the microstructure and achieve a redistribution of dopants [24,25]. An understanding of the deleterious effects of oxygen in both starting materials and incorporation during processing has led to improved electrical properties in Si-Ge alloys [26]. Computational modeling of the n-type Si-Ge system suggests that the optimum *ZT* at 1300 K is in the range of 1.1 to 1.2 [27] and 1.1 for p-type Si-Ge [28], although such high *ZT* values for p-type Si-Ge have not been widely confirmed by experimental observations. The *ZT* of standard phosphorus-doped n-type Si-Ge alloys prepared by zone levelling is 17–20% lower than the theoretical maximum. Analysis of the electrical characteristics of these alloys shows that a high carrier concentration (e.g., 3.5 to 4.2 $\times$ $10^{20}$ $cm^{-3}$) results in low electrical resistivity and electrical power factors close to the theoretically predicted maximum of 40 to 45 ($\mu W/(cm\text{-}K^2)$) at 873 K, a sharp decrease in the power factor is observed between 873 and 1273 K. This rapid decrease in the power factor causes a decrease in *ZT* at the highest temperatures, in addition to the onset of intrinsic conductivity during which the population of minority carriers also decreases the Seebeck coefficient while increasing the bi-polar thermal conductivity. Performance approaching the theoretical maximum is often observed in alloys exhibiting a moderate carrier concentration combined with high carrier mobility, which combine to produce a low resistivity with a high Seebeck coefficient, S, due to the logarithmic dependence of S on carrier concentration.

The microstructure is highly dependent on powder consolidation time and temperature (e.g., hot pressing or SPS parameters), and it is well-known that microstructure plays an important role in the electrical transport of these alloys due to the presence of electrical potential barriers at grain boundaries. For this reason, an understanding of the effect of impurities, an inevitable consequence of handling and processing the raw materials is important. Since oxygen is ubiquitous and highly reactive, its role is critical to the properties of the material. Despite considerable research on the role of oxygen in the silicon-based electronics industry, there has been minimal studies to understand its role on the thermoelectric performance of silicon germanium alloys. Neutron activation studies performed on cast and also on hot pressed $Si_{80}Ge_{20}$ showed that total oxygen content varies from 0.3 to 6.7 atomic percent (6). Silicon tends to oxidize more readily than germanium in a mixture of the two elements. As the silicon is oxidized, the formation of second phase oxides will shift the bulk composition of the alloy toward the germanium-rich end with a corresponding shift in the lattice parameter that can be quantified by x-ray diffraction. Oxygen contamination, whether in the starting materials or incorporated during processing, will degrade electrical mobility, which then lowers the power factor ($S^2\sigma$). Neutral second phase impurities can also reduce carrier mobility through impurity scattering and by increasing the magnitude of potential barriers at grain boundaries. Even relatively low exposure of the raw materials to oxygen can affect the sintering process and result in limited grain growth during consolidation with higher electrical resistivity, thus the need for tight controls on the purity of starting materials and on the processing environment. Thermal conductivity will also decrease as the concentration of neutral second phase impurities increases. While a significant amount of research during the last 20 years has focused on reducing the thermal conductivity of thermoelectric materials by grain size refinement, it

should be pointed out that since the mean free path of phonons decreases with temperature, the importance of grain size refinement for high temperature RTG applications in which portions of the material approach temperatures near 1300 K has to be weighed against effective phonon path length within the temperature range of interest. The use of nanostructured silicon–germanium raises the issue of phonon mean free path lengths that are less than the average grain size, i.e., providing no benefit over standard or fine-grained Si-Ge. Moreover, the carrier mean free path in Si-Ge is calculated to be on the order of 50 nm at 300 K, which suggests that mobility and, thus, electrical conductivity, might not be affected until the grain size is reduced below this value. However, there are reports demonstrating a 30 to 40 percent reduction in carrier mobility in ultra-fine grained Si-Ge (e.g., 100 nm to 300 nm) as a result of the presence of electrical potential barriers. This barrier height has been estimated at ~ $2.0 \times 10^{-8}$ Ω-cm$^2$. Maintaining a low oxygen environment is one of the most critical processing parameters to ensure consistently high-quality Si-Ge TE materials.

Depending on the processing approach, commercial silicon can contain high amounts of oxygen. Consequently, a chemical analysis and detailed records must be rigorously maintained and scrutinized during the lifetime of the program. Since carbon is ubiquitous its presence poses another challenge in the effort to optimize the performance of Si-Ge alloys. Fine-grained, high oxygen-content alloys can also contain copious amounts of carbon, on the order of 5 at. %, or comparable to the total oxygen content based on neutron activation. This amount of carbon can have an impact on grain growth, and the formation of SiC during sintering. It is therefore important that each lot of starting material should be scrutinized by the chemical analysis with respect to the maximum acceptable level of metal and non-metal impurities. It is also noteworthy that most chemical suppliers provide analysis upon request; however, the analysis is typically on a metals-basis, meaning non-metallic impurities, such as oxygen and carbon, are not routinely measured. A chemical analysis, starting with the vendor-supplied precursor materials and following through to the final diced TE legs, is one of the most important factors that will determine the quality and reproducibility of the synthesis process.

Considering the necessary chemical doping (P for n-type and B for p-type), there exists a well-documented 'metastability' in heavily doped Si-Ge alloys at elevated temperature due to precipitation of the dopants out of solution. This phenomenon has obvious implications for long-term power distribution. In measurements of the dependence of the carrier concentration on time at temperature, it has been found that heavily-doped n-type Si-Ge materials show a decrease of 40% in carrier concentration after only 70 min at 873 K and approach a limiting decrease in carrier concentration of ~74% after 4000 h [29]. As stated previously, moderately-doped Si-Ge alloys possessing a fine grain size (~800 nm to 10,000 nm) with ultra-low oxygen content offer the best potential for maximum *ZT* with the lowest degradation rate. Alloys with an average grain size in the range of 1 to 5 microns with room-temperature carrier concentration values of ~$2 \times 10^{20}$ cm$^{-3}$ had a mobility at or near the best values observed in zone leveled materials. Integrated average power factors of 35 μW/(cm-K$^2$) between 573 and 1273 K have routinely and reproducibly been produced using a solid state synthesis approach (to be discussed later).

Since the most prominent application for Si-Ge thermoelectric materials has been in the NASA MHW and GPHS RTG programs, a review of this material would be incomplete without including mention of the coating that was applied to the material as part of the unicouple assembly process. In the legacy MHW and GPHS applications for Si-Ge, the first-bond assembly (78% Si n and p legs and the hot shoe) and the alumina spacer are coated with a 1 micron thick layer of $Si_3N_4$ prior to the second bond processing step [30,31]. The purpose of the coating is to control sublimation of silicon from the hot shoe and hot ends of the pellets, which would otherwise lead to a range of problems, including electrical shorting, increased contact resistance, and decreased power output. Sublimation of TE materials result in geometry changes of the TE legs, e.g., typically a cross-sectional area reduction. In the absence of suppression control measures, the hot junction temperature increases because of sublimation, which in turn increases the rate of sublimation thereby resulting in

a cascade effect leading to catastrophic failure. Typically, materials exhibiting sublimation rates in excess of $5 \times 10^{-6}$ g/cm$^2$-h require some type of sublimation suppression measure to enable long-term operation at that temperature. Application of the coating reduces the rate of sublimation of the Si-Ge material from $4 \times 10^{-7}$ g/cm$^2$-h to $2 \times 10^{-8}$ g/cm$^2$-h at a temperature of 1273 K. The maximum allowable sublimation rate for any given hot junction temperature is based on maintaining the reduction in cross sectional area of the TE elements to the range of 5–10% after 14 years of operation at the maximum operating temperature. For the legacy Si-Ge unicouples at a hot junction temperature of 1273 K, a 5% reduction in leg area over 14 years requires that the sublimation rate not exceed $2 \times 10^{-7}$ g/cm$^2$/h while a 10% reduction in leg area allows for a maximum sublimation rate of $4 \times 10^{-7}$ g/cm$^2$/h. It is interesting to note that uncoated MHW Si-Ge could be used with a hot junction temperature of 1273 K if a 10% reduction in leg area would be tolerable. Nevertheless, minimization of sublimation reaction products in the uncouple-insulation area was a primary objective. Moreover, an understanding of the sublimation characteristics of the TE material and hot shoes was also essential for establishing RTG life performance prediction models. The coating was applied by CVD processing to the hot shoe-pellet assembly. The first bond assemblies and alumina spacer were CVD-coated in four cycles of 40 min duration each. Weight gain was used as a nondestructive means of determining overall $Si_3N_4$ coating thickness. Coating thickness was also measured by optical metallography on cross-sectioned Si-Ge pellets after coating and after unicouple assembly thermal cycling. Coating thickness typically ranged from 1.0 to 1.5 microns.

## 4. Efforts to Improve the Thermoelectric Properties of Si-Ge

Even though silicon–germanium has been thoroughly studied for over 50 years, research has continued to explore new mechanisms to further improve its performance. To establish a historical perspective, Figure 3 shows the temperature variation of *ZT* of legacy $Si_{78}Ge_{22}$ based on data from multiple sources [32–34]. The maximum *ZT* of the legacy n-type material is seen to occur at a temperature of 900 K with a magnitude of 0.96. The corresponding maximum *ZT* for the legacy p-type composition is 0.71 at a temperature of 1000 K. Since the late 1970s and early 1980s, these values have remained the benchmark for subsequent research to improve *ZT*. For an excellent overview of the transport properties of $Si_{80}Ge_{20}$ and the evolution of GaP as an additive, the reader is referred to a 1993 paper by Vining and Fleurial [35].

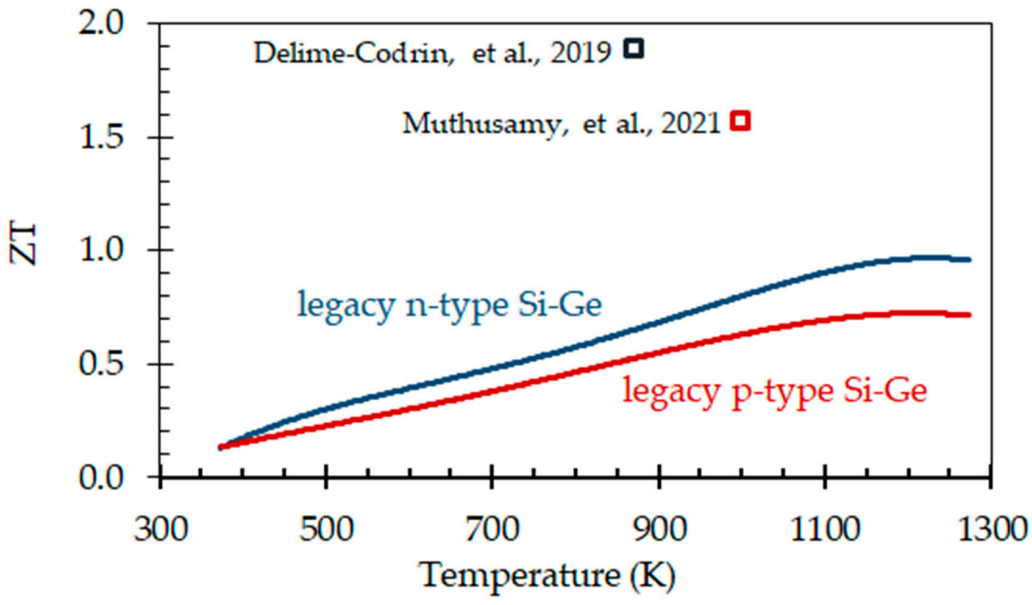


**Figure 3.** *ZT* vs. Temperature for n- and p-type legacy $Si_{78}Ge_{22}$. Examples of recent published results are shown for comparison.

From Equation (1), it is seen that increasing *ZT* requires one or more of the following: increasing the Seebeck coefficient, increasing electrical conductivity, or decreasing the thermal conductivity. We consider approaches to improve or enhance each of the three primary transport properties separately.

### *4.1. Thermal Conductivity*

As mentioned previously, during the 1980s and 1990s, efforts to improve Si-Ge focused primarily on thermal conductivity reduction by grain size refinement [36–41], guided by the Klemens–Callaway phenomenological model [42] for the high-temperature lattice thermal conductivity, which describes the conduction of heat by both transverse and longitudinal acoustic phonons as an approximation to the known phonon dispersion spectrum of silicon and Ge-Si alloys. Grain boundary scattering, which was a precursor to the now-familiar nanostructuring approach, was most effective at scattering intermediate-to-long wavelength lattice phonons when the grain size was reduced to the 0.1 to 10 μm range. Many studies reported a concomitant reduction in electrical conductivity that tended to offset the reduction in thermal conductivity. It should be noted that the association between grain size and lattice thermal conductivity gave rise to the model of an ideal thermoelectric material as a "phonon-glass electron-crystal" (PGEC), as envisioned by Slack in 1995 [43]. The PGEC concept, which remains the basis for much of current-day work on thermoelectric materials, is based on the idealized model of a material that conducts heat, like a glass, where in the limiting case a phonon is scattered after propagating one wavelength, combined with the electronic transport of a single crystal, where the absence of defects results in a maximization of carrier mobility. Striking the balance between minimal grain size and minimal depression of carrier mobility remains the goal of recent research on silicon–germanium [44–48]. Another approach at scattering intermediate wavelength phonons during the late 1980s and early 1990s was the incorporation of inert, second-phase inclusions [49–54]. The particles, typically oxides or nitrides in the 5 to 10 nm size range, were introduced by various means with the most noteworthy approach attributed to the ThermoElectron Corporation, where a spark erosion system was developed to co-produce particles of 2–12 nm Si-Ge along with various additives [55]. Perhaps the most promising approach at that time involved the introduction of $Si_3N_4$ into boron-doped p-type Si-Ge. Samples exhibited much lower total thermal conductivity values than standard Si-Ge by as much as 40% at room temperature, even following multiple high temperature anneals [56]. However, the synthesis process involved complicated and costly equipment and work was discontinued following the end of the Cassini program in the mid-1990s.

Silicon–germanium is a substitutional solid solution alloy with complete miscibility across the entire composition range and is therefore characterized by a varying degree of mass fluctuation scattering, depending on the Si:Ge ratio, resulting from point disruptions in the lattice periodicity as discussed by Abeles [57], Klemens [58], and White and Klemens [59], to cite only a few of the many papers devoted to this subject. Mass fluctuation, or point defect scattering, refers to scattering that occurs when a displacement wave encounters a zero dimensional disruption in the periodicity of the lattice. These features are also regarded to include dislocations (which are not strictly zero dimensional artifacts), impurities, and vacancies. Point defect scattering is most effective at short wavelength phonons, on the order of typical interatomic distances. While point defect scattering may be considered somewhat of an intrinsic characteristic of the alloy composition itself and not directly amenable to tuning, there have been recent efforts to investigate the effects of randomness of the constituent atoms throughout the alloy on the anharmonic scattering of low-frequency phonon modes [60]. This type of 'atomic engineering' approach for control of atom placement could, in principle, result in further reductions in the material's thermal conductivity.

The use of electric field assisted powder consolidation gained widespread acceptance in the mid-1990s as a means to sinter and densify powder with minimal grain growth. Since the current is passed directly through the powder rather than through heating

elements in conventional hot pressing, the use of this technique, referred to as Spark Plasma Sintering or Field Assisted Sintering Technology, has surpassed conventional hot pressing because of its ability to provide higher heating rates and shorter sintering times, which are necessary in order to retain sub-micron microstructures in the final product. Reports of the use of SPS/FAST consolidation with Si-Ge alloys first appeared in 1997–1998 [61,62] and worldwide interest rapidly grew following these initial studies. The majority of the subsequent work involving the use of SPS/FAST for consolidation of bulk Si-Ge alloys have been focused on achieving sub-micron grain size (nano-bulk materials) and a reduction in thermal conductivity [63–69], although there are also reports of improved mechanical properties (hardness, fracture toughness) resulting from a more refined microstructure than possible through conventional hot pressing [66].

A review of silicon–germanium for thermoelectric applications would not be complete without a mention of the role of gallium phosphide. Considerable experimental and theoretical efforts were applied to develop advanced Si-Ge alloys containing this III-V compound during the 1980s and early 1990s. It is generally regarded that the inspiration for this effort can be traced to work at Syncal Corporation in the late 1970s that showed significant reduction in the thermal conductivity of Si-Ge alloys containing varying amounts of GaP [70]. These reports claimed up to a 50% reduction in thermal conductivity than in comparable materials without GaP. This disruptive announcement propelled numerous groups to focus on GaP-containing alloys, including an aggressive DOE-sponsored thermoelectric multicouple program referred to as MOD-RTG [71], which included use of SiGe/GaP in the n-type legs in addition to other novel and radical design constructs that were based on work performed at Fairchild [72]. What was particularly interesting about the results is that the addition of GaP to Si-Ge should not, by itself, result in a lower thermal conductivity than that of the simple binary alloy, since the atomic masses of Ga and P both lie between those of Si and Ge, there should be no contribution to the material's mass fluctuation scattering. Adding GaP to Si-Ge should actually *decrease* the effective mass fluctuation scattering term. It was subsequently determined that the cause of the reduced thermal conductivity was the result of how the GaP-containing materials were processed. The addition of GaP to Si-Ge required additional grinding steps, which resulted in finer starting particle sizes and ultimately a finer grain size in the hot pressed alloys. The conclusion was that standard Si-Ge alloys processed in a similar manner would exhibit similar reduction in thermal conductivity. It should also be noted that there was never a clear indication that the equilibrium (i.e., thermally stabilized) *ZT* of GaP-containing alloys was superior to that of the standard, legacy material.

### *4.2. Seebeck Coefficient*

Recent research to improve the Seebeck coefficient of Si-Ge has included the study of quantum confinement in low dimensional systems, which was initially advanced by Hicks and Dresselhaus in 1993 [73]. The approach is based on the relationship between the Seebeck coefficient and the rate of change of the density of states with energy, or in other words, the Seebeck coefficient is proportional to the local slope of the density of states curve with respect to energy. In a quantum well structure, the density of states would have sharp features at the interfaces, thereby leading to an enhancement in the Seebeck coefficient. Another intriguing approach for increasing the Seebeck coefficient in thermoelectric materials is electron energy filtering. The basis for energy filtering stems from a carrier's contribution to the total Seebeck coefficient as a function of its energy; higher-energy electrons contribute more to a material's Seebeck coefficient than lower-energy electrons. When the lower energy carriers are preferentially scattered by a suitable potential barrier, the overall Seebeck coefficient is increased. These barriers can be scattering centers or grain boundaries where the potential energy associated with the artifact must exceed that of the lower energy carriers and less than that of the higher energy carriers. This approach can be effective when the characteristic separation distance between successive potential barriers is less than the mean free path of the charge carriers, otherwise

the temperature-dependent scattering rate would act as the dominant mechanism. This imposes an obvious complication with high-temperature materials, such as Si-Ge, since thermal diffusion effects have the potential to relax nanostructured features required for energy filtering. Moreover, some studies suggest that energy filtering is more effective at low doping levels than for material that are heavily-doped (i.e., degenerate systems), such as Si-Ge, where the Schottky barriers in grain boundaries are small and, thus, have insignificant impact on *ZT* [74]. Energy filtering in bulk Si-Ge may prove to be useful in limited circumstances, for example, where porosity in high-density, nanograined materials result in a sufficiently enhanced Seebeck coefficient and reduced lattice thermal conductivity to overcome an increase in electrical resistivity [75].

Modulation doping offers another path toward improved thermoelectric performance. Modulation doping evolved from earlier applications in thin-film semiconductors for which charge carriers are separated from the dopant atoms responsible for ionized impurity scattering that reduce mobility and increase electrical resistivity [76–78]. Early efforts achieved this separation of carriers from ionized scattering centers by forming structures comprised of alternating layers of undoped conducting channels and doped donor channels where, in some configurations, these two channels were separated by an undoped conducting channel. Typically, these structures were prepared using thin film technology, such as molecular beam epitaxy. Adaptation to bulk, 3D materials has taken the form of nanocomposites, where suitable nanoparticles are dispersed within a host matrix. One particularly promising study involved a matrix phase of $Si_{95}Ge_5$ with $Si_{70}Ge_{30}P_3$ as the dispersed, nanoparticle phase [79]. This study reported a 30–40% higher *ZT* than "equivalent" optimally-doped Si-Ge due to a decreased electrical resistivity, decreased thermal conductivity, and an unchanged Seebeck coefficient. Another study claimed energy filtering as the mechanism responsible for a high *ZT* of 1.3 at 1100 K in p-type Si-Ge with $TiO_2$ inclusions [80]. Addition work is needed in order to fully understand the extent to which 3D implementations of this approach can be implemented in bulk Si-Ge.

Combining multiple optimization pathways, such as nanostructuring with energy filtering or band structure modification, offers the potential to achieve increases in *ZT* beyond that of a single mechanism. Two recent papers report the results of preparing nanostructured Si-Ge alloys to which electronic structure modifications were introduced. Delime-Codrin et al. [81] prepared nanostructured n-type $Si_{0.55}Ge_{0.35}$ alloys with a remarkable thermal conductivity of 0.80 W $m^{-1}$ $K^{-1}$ at $T < 873$ K. Their density functional theory calculations predicted an increase in Seebeck coefficient by addition of iron atoms, and a Seebeck coefficient of >517 was reported in $Si_{0.55}Ge_{0.35}(P_{0.10}Fe_{0.01})$ at 673 K. As a result of this combination of enhancements, the authors claim a maximum *ZT* of 1.88 at 873 K. In another study, Muthusamy et al. [82] prepared $Si_{0.65-x}Ge_{0.32}Ni_{0.03}B_x$ with x = 0.01, 0.02, 0.03, and 0.04 by high energy milling combined with high-pressure, low-temperature sintering. The introduction of a 3D transition metal element as a source of impurity states in the electronic density of states was the motivation for the addition of nickel. As a result, a *ZT* of 1.56 was found at 1000 K for x = 0.03 from a thermal conductivity of 1.47 W $m^{-1}$ $K^{-1}$, a Seebeck coefficient of 321 $\mu VK^{-1}$, and a resistivity of 4.49 m$\Omega$-cm. The authors report a lattice thermal conductivity of 0.91 W $m^{-1}$ $K^{-1}$ in this sample. Because of the limited solubility of Ni in both Ge and Si, the effect of second phase intermetallic compounds, such as $Ge_2Ni$, $GeNi_{1.5}$ must be considered in addition to oxygen effects and the presence of neutral complexes, such as $GeO_2$. While the $S^2\sigma$ product in these samples is unremarkable, the astonishing decrease in thermal conductivity, if verified by independent studies, would represent a significant breakthrough in the thermoelectric performance of Si-Ge alloys.

## 5. Outlook

Silicon-rich Si-Ge alloys have dominated the domain of high-temperature thermoelectric research and development efforts for over half a century. The unique combination of a favorable and tunable energy band gap, sufficient solid solubility of n- and p-type substitutional dopants to obtain good thermoelectric properties, and predictable sublimation and

electrical characteristics, have made these the materials-of-choice for radioisotope power onboard robotic outer planetary missions since the Pioneer and Voyager era. Modern-day circuit designers are finding Si-Ge alloys to be more efficient than silicon in terms of power consumption and performance. New approaches for improving the figure-of-merit in bulk materials are finding their way into Si-Ge research and it is likely that this area will remain a robust field for additional future research and new applications. NASA has selected Si-Ge as the thermoelectric material to be used in the Next-Generation RTG program. Future NASA RTG missions will be required to use a step 2 GPHS design, which contains a thicker fine-weave pierced fabric graphite aeroshell, designed to increase the safety margin in the event of a reentry and impact event. The increased thickness of the step 2 aeroshell limits the number of GPHS modules to 16, compared with 18 modules in the legacy Cassini RTG. This reduces the available thermal inventory to 244 watts at the beginning of the mission, compared with 285 watts in the legacy RTG. The reduction in available heat will likely accelerate efforts to improve the *ZT* of both n- and p-type compositions. Recent claims of *ZT* values greater than unity in both n- and p-type Si-Ge will no doubt stimulate further research to validate these claims and investigate the stability of the nanostructuring and band structure modifications with long-term thermal aging studies. Alternate materials such as Skutterudites paired with n-type $La_{3-x}Te_x$ and p-type Zintl phase materials, such as $Yb_{14}MnSb_{11}$ or $Yb_{14}MgSb_{11}$ in a segmented design, could outperform Si-Ge. However, before legacy Si-Ge can be replaced in a critical, high-profile mission, any changes will need to undergo extensive, long-term testing to fully understand and mitigate any chemical and microstructural changes that may occur during a mission that could potentially last for 40+ years, as evidenced by the Voyager 1 and 2 probes.

**Funding:** This research received no external funding.

**Institutional Review Board Statement:** This study did not require ethical approval.

**Informed Consent Statement:** Not applicable.

**Data Availability Statement:** This study did not report new or original data.

**Conflicts of Interest:** The author declares no conflict of interest.

## References and Notes

1. Available online: https://voyager.jpl.nasa.gov/mission/status/ (accessed on 28 March 2022).
2. Pitrolo, A.; Morrow, R.; Arker, A. Multihundred Watt Radioisotope Thermoelectric Generator (MHW-RTG). In Proceedings of the Intersociety Energy Conversion Engineering Conference, Boston, MA, USA, 3 August 1971; New York Society of Automotive Engineers, Inc.: New York, NY, USA, 1971; pp. 492–511.
3. "Thermopower" refers to the magnitude of the (open circuit) voltage for a given temperature difference, T. "Seebeck coefficient" refers to the slope of the ΔV vs. ΔT curve.
4. Cammarata, A. Phonon–phonon scattering selection rules and control: An application to nanofriction and thermal transport. *R. Soceity Chem. (RSC) Adv.* **2019**, *9*, 37491–37496. [CrossRef]
5. Bennet, G. The Selenide Saga: A Contribution toward a History of the Selenide Isotope Generator. In Proceedings of the 14th International Energy Conversion Engineering Conference—Propulsion and Energy Forum, Salt Lake City, UT, USA, 25–27 July 2016.
6. Brunenkant, E.J. (Ed.) *SNAP Nuclear Space Reactors*; Library of Congress Catalog Card Number 66-62772; U.S. Atomic Energy Commission Division of Technical Information: Washington, DC, USA, 1966. Available online: https://www.osti.gov/ (accessed on 28 March 2022).
7. During the Cassini program a suggestion was advanced to substitute a water cooled Cu "pancake" mold for the Cu block finger mold. The rationale was that the pancake mold would result in more uniform and reproducible casting conditions and a casting weight more compatible with the weight of the subsequent hot pressed compacts. However, subsequent work revealed significant differences in the Si-Ge transport properties so the larger pancake mold was never adopted.
8. Abeles, B.; Beers, D.; Cody, G.; Dismukes, J. Thermal Conductivity of Ge-Si Alloys at High Temperatures. *Phys. Rev.* **1962**, *125*, 44. [CrossRef]
9. Dismukes, J.; Ekstrom, L.; Steigmeier, E.; Kudman, I.; Beers, D. Thermal and Electrical Properties of Heavily Doped Ge-Si Alloys up to 1300 K. *J. Appl. Phys.* **1964**, *35*, 2899. [CrossRef]
10. Hassion, F.X.; Goss, A.J.; Trumbore, F.A. On the Germanium-Silicon phase diagram. *J. Phys. Chem.* **1955**, *59*, 1118–1119. [CrossRef]
11. Trumbore, F.A. Solid Solubilities of Impurity Elements in Germanium and Silicon. *Bell Syst. Tech. J.* **1960**, *39*, 205–233. [CrossRef]

12. Rowe, D.M.; Savvides, N. The reversal of precipitation in heavily doped silicon-germanium alloys. *J. Phys. D: Appl. Phys.* **1979**, *12*, 1613. [CrossRef]
13. Nasby, R.D.; Burgess, E.L. Precipitation of Dopants in Silicon-Germanium Thermoelectric Alloys. *J. Appl. Phys.* **1972**, *43*, 2908–2909. [CrossRef]
14. Raag, V. Dopant precipitation in silicon—germanium alloys. In Proceedings of the 7th Intersociety Energy Conversion Engineering Conference, San Diego, CA, USA, 25 September 1972.
15. Olesinski, R.W.; Abbaschian, G.J. The Ge−Si (Germanium-Silicon) system. *Bull. Alloy. Phase Diagr.* **1984**, *5*, 180–183. [CrossRef]
16. Lee, M.G.; Kim, S.J. Elastic-plastic constitutive model for accurate springback prediction in hot press sheet forming. *Met. Mater. Int.* **2012**, *18*, 425–432. [CrossRef]
17. Lü, L.; Lai, M.O. Introduction to Mechanical Alloying. In *Mechanical Alloying*; Springer: Boston, MA, USA, 1998.
18. Suryanarayana, C. Mechanical Alloying: A Novel Technique to Synthesize Advanced Materials. *AAAS Res.* **2019**, *2019*, 4219812. [CrossRef]
19. Gilman, P.S.; Benjamin, J.S. Mechanical Alloying. *Annu. Rev. Mater. Sci.* **1983**, *13*, 279–300. [CrossRef]
20. Froes, F.H. *Mechanical Alloying*; AccessScience, McGraw-Hill Education: New York, NY, USA, 2020.
21. Arzt, E.; Schultz, L. New Materials by Mechanical Alloying Techniques. *Mater. Manuf. Processes* **1991**, *6*, 733–736. [CrossRef]
22. Cook, B.A.; Harringa, J.L.; Han, S.H. Preparation of Thermoelectric Materials by Mechanical Alloying. In *CRC Handbook on Thermoelectrics—Chapter 12*; Rowe, D.M., Ed.; CRC Press: Boca Raton, FL, USA, 1995.
23. Cook, B.A.; Harringa, J.L. Solid State Synthesis of Thermoelectric Materials. In *CRC Handbook of Thermoelectrics*; Taylor & Francis: Boca Raton, FL, USA, 2006; pp. 19-1–19-14.
24. Shukla, V.S.; Rowe, D.M. The effect of short-term heat treatment on the thermoelectric properties of heavily doped n-type silicon germanium alloys. *Appl. Energy* **1981**, *9*, 131–137. [CrossRef]
25. Vandersande, J.W.; Wood, C.; Draper, S.L.; Raag, V.; Alexander, M.; Masters, R. Improved GaP doped SiGe thermoelectric material. In Proceedings of the Transactions of the Fifth Symposium on Space Nuclear Power Systems, Albuquerque, NM, USA, 11 January 1988; pp. 629–632.
26. Cook, B.A.; Harringa, J.L.; Han, S.H.; Beaudry, B.J. Parasitic effects of oxygen on the thermoelectric properties of $Si_{80}Ge_{20}$ doped with GaP and P. *J. Appl. Phys.* **1992**, *72*, 1423–1428. [CrossRef]
27. Vining, C.B. A model for the high-temperature transport properties of heavily doped n-type silicon-germanium alloys. *J. Appl. Phys.* **1991**, *69*, 331–341. [CrossRef]
28. Ahmad, S.; Singh, A.; Basu, R.; Vitta, S.; Muthe, K.P.; Gadkari, S.C.; Gupta, S.K. Optimization of Thermoelectric Properties of Mechanically Alloyed p-Type SiGe by Mathematical Modelling. *J. Electron. Mater.* **2019**, *48*, 649–655. [CrossRef]
29. Cook, B.A.; Harringa, J.L.; Han, S.H.; Alexander, C.; Beaudry, B.J.; Gschneidner, K.A., Jr. *Radioisotope Power Systems Support Program—Advanced Thermal-to-Electrical Conversion Materials*, Ames Laboratory Quarterly Progress Report to U.S. Department of Energy Office of Special Applications; 31 March 1995, unpublished.
30. Stapfer, G.; Truscello, V.C. Sublimation behavior of silicon nitride/$Si_3N_4$/coated silicon germanium/SiGe/unicouples. In Proceedings of the 10th Intersociety Energy Conversion and Engineering Conference, Newark, DE, USA, 17 August 1975.
31. Nakahara, J.F.; DeFillipo, L.E. Sublimation Characteristics of Silicon Nitride Coated SiGe and SiMo Unicouple Components. In Proceedings of the XI International Conference on Thermoelectrics, Arlington, TX, USA, 7–9 October 1992.
32. Raag, V. Comprehensive Thermoelectric Properties of n- and p-type 78% Si—22% Ge Alloy. In Proceedings of the 2nd International Conference on Thermoelectric Energy Conversion, University of Texas, Arlington, TX, USA, 22–24 March 1978.
33. RCA Topical Report. *Silicon Germanium Thermoelectric Materials and Module Development Program*; U.S. AEC Research and Development Report Category UC33 TID 4500 Contract AT (29—2)—2910, 1 January 1968 to 1 November 1969; Clearinghouse for Federal Scientific and Technical Information, National Institute of Standards and Technology, U S Department of Commerce: Springfield, VA, USA, 1968.
34. JPL Database. Standard SiGe Thermoelectric Processes. Unpublished work. 1976.
35. Vining, C.B.; Fleurial, J.P. Silicon-Germanium: An Overview of Recent Developments. In Proceedings of the Tenth Symposium on Space Nuclear Power and Propulsion, Albuquerque, NM, USA, 10–14 January 1993.
36. Meddins, H.R.; Parrott, J.E. The thermal and thermoelectric properties of sintered germanium-silicon alloys. *J. Phys. C Solid State Phys.* **1976**, *9*, 1263. [CrossRef]
37. Rowe, D.M. Theoretical optimization of the thermoelectric figure of merit of heavily doped hot-pressed germanium-silicon alloys. *J. Phys. D Appl. Phys.* **1974**, *7*, 1843. [CrossRef]
38. Rowe, D.M.; Bhandari, C.M. Effect of grain size on the thermoelectric conversion efficiency of semiconductor alloys at high temperature. *Appl. Energy* **1980**, *6*, 347–351. [CrossRef]
39. Rowe, D.M.; Shukla, V.S. The effect of phonon-grain boundary scattering on the lattice thermal conductivity and thermoelectric conversion efficiency of heavily doped fine-grained, hot-pressed silicon germanium alloy. *J. Appl. Phys.* **1981**, *52*, 7421–7426. [CrossRef]
40. Slack, G.A.; Hussain, M.A. The maximum possible conversion efficiency of silicon-germanium thermoelectric generators. *J. Appl. Phys.* **1991**, *70*, 2694–2718. [CrossRef]
41. Hua, C.; Minnich, A.J. Importance of frequency-dependent grain boundary scattering in nanocrystalline silicon and silicon–germanium thermoelectrics. *Semicond. Sci. Technol.* **2014**, *29*, 124004. [CrossRef]

42. Callaway, J. Model for lattice thermal conductivity at low temperatures. *Phys. Rev.* **1959**, *113*, 1046–1051. [CrossRef]
43. Slack, G.A. *CRC Handbook of Thermoelectrics*; Rowe, D.M., Ed.; CRC: Boca Raton, FL, USA, 1995; p. 407.
44. Upadhyaya, M.; Khatami, S.N.; Aksamija, Z. Engineering thermal transport in Si-Ge-based nanostructures for thermoelectric applications. *J. Mater. Res.* **2015**, *30*, 2649–2662. [CrossRef]
45. Taborda, J.P.; Romero, J.J.; Abad, B.; Muñoz-Rojo, M.; Mello, A.; Briones, F.; Gonzalez, M.M. Low thermal conductivity and improved thermoelectric performance of nanocrystalline silicon germanium films by sputtering. *Nanotechnology* **2016**, *27*, 175401. [CrossRef] [PubMed]
46. Lan, Y.; Wang, D.; Ren, Z. Silicon–Germanium Alloys. In *Advanced Thermoelectrics: Materials, Contacts, Devices, and Systems*; Ren, Z., Lan, Y., Zhang, Q., Eds.; CRC Press, Taylor & Francis Group: Boca Raton, FL, USA, 2018; pp. 353–371. ISBN 9781498765725.
47. Tukmakova, A.; Novotelnova, A.; Samusevich, K.; Usenko, A.; Moskovskikh, D.; Smirnov, A.; Mirofyanchenko, E.; Takagi, T.; Miki, H.; Khovaylo, V. Simulation of field assisted sintering of silicon germanium alloys. *Materials* **2019**, *12*, 570. [CrossRef] [PubMed]
48. Das, P.; Bathula, S.; Gollapudi, S. Evaluating the effect of grain size distribution on thermal conductivity of thermoelectric materials. *Nano Express* **2020**, *1*, 020036. [CrossRef]
49. Beaty, J.S.; Rolfe, J.L.; Vandersande, J.W. Thermoelectric Properties of Hot-Pressed Ultra-Fine Particulate Si-Ge Powder Alloys with Inert Additions. *MRS Online Proc. Libr.* **1991**, *234*, 105–109. [CrossRef]
50. Scoville, N.; Bajgar, C.; Rolfe, J.; Fleurial, J.P.; Vandersande, J. Status of Thermal Conductivity Reduction in Si-Ge Using Ultrafine Particulates. In Proceedings of the Eleventh Conference on Space Nuclear Power and Propulsion, Albuquerque, NM, USA, 9–13 January 1994; Volume 301, pp. 505–510.
51. Cook, B.A.; Harringa, J.L.; Loughin, S. Fullerite additions as a phonon scattering mechanism in p-type Si-20 at. % Ge. *Mater. Sci. Eng. B* **1996**, *41*, 280–288. [CrossRef]
52. Borshchevsky, A.; Fleurial, J.P.; Vandersande, J. Experimental approaches for improving Si-Ge thermoelectric efficiency at JPL. In Proceedings of the 25th Intersociety Energy Conversion Engineering Conference (IECEC-90), Reno, NV, USA, 12–17 August 1990; Volume 2, pp. 397–401.
53. Wang, Z.; Chen, H.; Chu, Y.; Cheng, Y.; Zhu, L.; Jian, X.Y.; Yu, H.J. Thermoelectric Properties P-Type Si-20 at. % Ge by Addition of TiN Nanoparticles. In *Materials Science Forum*; Trans Tech Publications Ltd.: Bäch, Switzerland, 2009; Volume 610, pp. 399–402.
54. Fatima, K.; Song, X.; Maryam, A.; Rasheed, M.N.; Iqbal, F.; Monakhov, E.V.; Asghar, M. Influence of environment on thermoelectric properties of n-type silicon-germanium alloy. *Dig. J. Nanomater. Biostructures (DJNB)* **2021**, *16*, 907–913.
55. Beaty, J.S.; Rolfe, J.L.; Vandersande, J.W. Properties of 100 Å P-Type Atomclusters and Thermoelectric Material. In Proceedings of the 25th Intersociety Energy Conversion Engineering Conference, Reno, NV, USA, 12–17 August 1990; Nelson, P.A., Schertz, W.W., Till, R.H., Eds.; American Institute of Chemical Engineers: New York, NY, USA, 1990; Volume 2, pp. 379–381.
56. Beaty, J.S.; Rolfe, J.L.; Vandersande, J.W. Thermoelectric Properties of Hot-Pressed Ultra-Fine Particulate Si-Ge Powder Alloys with Inert Additions. In *Modern Perspectives on Thermoelectrics and Related Materials*; Allred, D.D., Vining, C.B., Slack, G.A., Eds.; Materials Research Society: Pittsburgh, PA, USA, 1991; pp. 105–110.
57. Abeles, B. Lattice Thermal Conductivity of Disordered Semiconductor Alloys at High Temperatures. *Phys. Rev.* **1963**, *131*, 1906. [CrossRef]
58. Klemens, P.G. Thermal resistance due to isotopic mass variation. *Proc. Phys. Soc.* **1957**, *A70*, 833. [CrossRef]
59. White, D.P.; Klemens, P.G. Thermal conductivity of thermoelectric Si0.8Ge0.2 alloys. *J. Appl. Phys.* **1992**, *71*, 4258–4263. [CrossRef]
60. Lee, Y.; Pak, A.; Hwang, G. What is the thermal conductivity limit of silicon germanium alloys. *Phys. Chem. Chem. Phys.* **2016**, *18*, 19544. [CrossRef]
61. Noguchi, T. Powder processing of thermoelectric materials-focusing on Si-Ge with new sintering technique. In Proceedings of the 16th International Conference on Thermoelectrics (XVI ICT'97) (Cat. No. 97TH8291), Dresden, Germany, 26–29 August 1997; pp. 207–214.
62. Noguchi, T.; Masuda, T.; Nitta, J. Study on diffusion barriers of doping elements in Si-Ge alloys. In Proceedings of the Seventeenth International Conference on Thermoelectrics (ICT98) (Cat. No. 98TH8365), Nagoya, Japan, 28 May 1998; pp. 406–409.
63. Thompson, D.; Hitchcock, D.; Lahwal, A.; Tritt, T.M. Single-element spark plasma sintering of silicon germanium. *Emerg. Mater. Res.* **2012**, *1*, 299–305. [CrossRef]
64. Bathula, S.; Gahtori, B.; Jayasimhadri, M.; Tripathy, S.K.; Tyagi, K.; Srivastava, A.K.; Dhar, A. Microstructure and mechanical properties of thermoelectric nanostructured n-type silicon-germanium alloys synthesized employing spark plasma sintering. *Appl. Phys. Lett.* **2014**, *105*, 061902. [CrossRef]
65. Zhu, Z.Y.; Guo, S.L. Thermoelectric properties of silicon germanium alloy nanocomposite fabricated by mechanical alloying and spark plasma sintering. In *Key Engineering Materials*; Trans Tech Publications Ltd.: Bäch, Switzerland, 2016; Volume 703, pp. 70–75.
66. Murugasami, R.; Vivekanandhan, P.; Kumaran, S.; Kumar, R.S.; Tharakan, T.J. Densification and alloying of ball milled Silicon-Germanium powder mixture during spark plasma sintering. *Adv. Powder Technol.* **2017**, *28*, 506–513. [CrossRef]
67. Vivekanandhan, P.; Murugasami, R.; Kumaran, S. Spark plasma assisted in-situ phase evolution and densification of nano-crystalline magnesium silicide–silicon germanium thermo-electric composite: Pulse current effects and densification mechanisms. *Scr. Mater.* **2018**, *146*, 344–348. [CrossRef]

68. Murugasami, R.; Vivekanandhan, P.; Kumaran, S.; Kumar, R.S.; Tharakan, T.J. Simultaneous enhancement in thermoelectric performance and mechanical stability of p-type Si-Ge alloy doped with Boron prepared by mechanical alloying and spark plasma sintering. *J. Alloys Compd.* **2019**, *773*, 752–761. [CrossRef]
69. Vishwakarma, A.; Chauhan, N.S.; Bhardwaj, R.; Johari, K.K.; Dhakate, S.R.; Gahtori, B.; Bathula, S. Melt-Spun Si-Ge Nano-Alloys: Microstructural Engineering Towards High Thermoelectric Efficiency. *J. Electron. Mater.* **2021**, *50*, 364–374. [CrossRef]
70. Pisharody, R.K.; Garvey, L.P. Modified Silicon-Germanium Alloys with Improved Performance. In Proceedings of the 13th Intersociety Energy Conversion Engineering Conference, San Diego, CA, USA, 20–25 August 1978; American Institute of Chemical Engineers: New York, NY, USA, 1978; pp. 1963–1968.
71. Modular Radioisotope Thermoelectric Generator (RTG) Program (1983–1991) US-DOE Contract number DE-AC01-83NE-32112. Available online: https://www.osti.gov/servlets/purl/10151769 (accessed on 31 March 2022). [CrossRef]
72. Schock, A. Revised MITG Design, Fabrication Proceedure, and Performance Predicitons. In Proceedings of the 13th Intersociety Energy Conversion Engineering Conference, San Diego, CA, USA, 20–25 August 1983; American Institute of Chemical Engineers: New York, NY, USA, 1983; pp. 1093–1101.
73. Hicks, L.D.; Dresselhaus, M.S. Effect of quantum-well structures on the thermoelectric figure of merit. *Phys. Rev. B* **1993**, *47*, 12727. [CrossRef]
74. Bachmann, M.; Czerner, M.; Heiliger, C. Ineffectiveness of energy filtering at grain boundaries for thermoelectric materials. *Phys. Rev. B* **2012**, *86*, 115320. [CrossRef]
75. Lee, H.; Vashaee, D.; Wang, D.Z.; Dresselhaus, M.S.; Ren, Z.F.; Chen, G. Effects of nanoscale porosity on thermoelectric properties of Si-Ge. *J. Appl. Phys.* **2010**, *107*, 094308. [CrossRef]
76. Dingle, R.; Störmer, H.L.; Gossard, A.C.; Wiegmann, W. Electron mobilities in modulation-doped semiconductor heterojunction superlattices. *Appl. Phys. Lett.* **1978**, *33*, 665. [CrossRef]
77. Daembkes, H. *Modulation-Doped Field-Effect Transistors: Principles, Design, and Technology*, 2nd ed.; IEEE Press: New York, NY, USA, 1991.
78. Schäffler, F. High-mobility Si and Ge structures. *Semicond. Sci. Technol.* **1997**, *12*, 1515. [CrossRef]
79. Ren, Z. Enhancement of Thermoelectric Properties by Modulation-Doping in Silicon Germanium Alloy Nanocomposites. *Nano Lett.* **2012**, *12*, 2077–2082. [CrossRef]
80. Ahmad, S.; Basu, R.; Sarkar, P.; Singh, A.; Bohra, A.; Bhattacharya, S.; Bhatt, R.; Meshram, K.N.; Samanta, S.; Gadkari, S.C.; et al. Enhanced thermoelectric figure-of-merit of p-type Si-Ge through $TiO_2$ nanoinclusions and modulation doping of boron. *Materialia* **2018**, *4*, 147–156. [CrossRef]
81. Delime-Codrin, K.; Omprakash, M.; Ghodke, S.; Sobota, R.; Adachi, M.; Kiyama, M.; Matsuura, T.; Yamamoto, Y.; Matsunami, M.; Takeuchi, T. Large figure of merit $ZT$ = 1.88 at 873 K achieved with nanostructured $Si_{0.55}Ge_{0.35}(P_{0.10}Fe_{0.01})$. *Appl. Phys. Express* **2019**, *12*, 045507. [CrossRef]
82. Muthusamy, O.; Singh, S.; Hirata, K.; Kuga, K.; Harish, S.K.; Shimomura, M.; Adachi, M.; Yamamoto, Y.; Matsunami, M.; Takeuchi, T. Synergetic Enhancement of the Power Factor and Suppression of Lattice Thermal Conductivity via Electronic Structure Modification and Nanostructuring on a Ni- and B-Codoped p-Type Si–Ge Alloy for Thermoelectric Application. *ACS Appl. Electron. Mater.* **2021**, *3*, 5621–5631. [CrossRef]